Synthesis of Conductive Nanocomposites by Selective In Situ Polymerization of Pyrrole within the Lamellar Microdomains of a Block Copolymer

M. C. de Jesus[†] and R. A. Weiss*[,†,‡]

Polymer Science Program and Department of Chemical Engineering, University of Connecticut, Storrs, Connecticut 06269-3136

S. F. Hahn

Central Research, The Dow Chemical Company, Midland, Michigan 48674

Received November 13, 1997; Revised Manuscript Received January 23, 1998

ABSTRACT: Electrically conductive nanocomposites were prepared by a selective in situ polymerization of pyrrole within the lamellae ionomeric microdomains of sulfonated poly(styrene-*b*-(ethylene-*alt*-propylene)), SEP, diblock copolymers. A conductivity of 10^{-3}−10^{-1} S/cm was achieved parallel to the film surface for PPy concentrations from 5 to 11 wt % PPy. Although the microstructure of the block copolymer was not purposefully aligned, the conductivity was anisotropic, varying 1−2 orders of magnitude parallel and normal to the plane of the composite films. The in situ polymerization of pyrrole in the SPS microphase did not disrupt the texture of the block copolymer microstructure, though the interphase between the polystyrene and rubber lamellae became more diffuse. Incorporation of PPy also improved the modulus of the block copolymer above the T_g of the ionomer microdomains.

Introduction

One approach for exploiting the intrinsic electrical conductivity of polymers such as polypyrrole, polythiophene, or polyaniline and overcoming their poor mechanical properties is to blend them with a nonconductive polymer. Over the past decade, many research groups have prepared conductive blends or composites by employing an in situ polymerization of the conductive polymer within a preformed polymer host using that approach, and that subject was recently reviewed.[1]

A variation on the blend theme is to use the mesophase texture of a block copolymer as a template for directly preparing an anisotropically conductive material. The key feature of that approach is that self-assembly of a block copolymer provides nanometer-size domains with well-defined geometries and spatial register, e.g., cubic packed spheres, hexagonal packed cylinders, and alternating lamellae.[2] The incorporation of conductive particles or the in situ polymerization of a conductive polymer within one of the microphases of a block copolymer produces a conductive *nanocomposite*.

Ishizu et al.[3,4] prepared anisotropically semiconducting films by exposing a poly(styrene-*b*-2-vinylpyridine) diblock copolymer (S2VP) with oriented lamellar microdomains to alkyl halide vapors, and they observed an 8 order of magnitude difference in the conductivity parallel and perpendicular to the plane of the resultant film. They also introduced colloidal silver into quarternized 2VP lamellae by the reduction of silver iodide.[5] Similarly, Stankovic et al.[6] incorporated iodine into a S2VP block copolymer, but they observed no relationship between the conductivity and the orientation of the block copolymer. Ishizu and co-workers[7] also used cross-linked S2VP films containing Cu(II) complexed to the 2VP for an in situ polymerization of pyrrole. Because the Cu(II) oxidant was only present in the 2VP microphase, polypyrrole (PPy) was restricted to the 2VP lamellar microdomains, and those materials had an electrical conductivity as high as 10^{-1} S/cm and high anisotropic conductivity. Smith et al.[8] prepared highly ordered nanocomposites containing poly(*p*-phenylenevinylene), PPV, another conductive polymer that exhibits photoluminescence, by polymerizing lyotropic liquid crystals to form a highly ordered matrix phase. The resulting hexagonally ordered PPV nanocomposite exhibited significantly enhanced photoluminescence.

Radhakrishnan and Saini[9] polymerized pyrrole in a poly(styrene-*b*-butadiene-*b*-styrene) (SBS) triblock copolymer using $FeCl_3$ as the oxidant and dopant. Although they claimed that the PPy was preferentially incorporated in the polybutadiene microdomains, the data presented in their paper do not support that conclusion. Their assertion of intercalation of PPy in the rubber domains was based upon optical microscopy and wide-angle X-ray diffraction, WAXD, but optical microscopy cannot resolve the 10−100 nm-sized microdomains that are characteristic of a block copolymer microstructure and WAXD probes a size scale 1−2 orders of magnitude smaller than that for the polybutadiene microdomains. Their optical micrographs clearly show macroscopically phase-separated PPy distributed throughout the polymer sample, which is typical of the product one obtains from an in situ oxidative polymerization of pyrrole in a polymer matrix that does not specifically interact with PPy.

The objective of the research described in the present paper was to preferentially incorporate PPy into the glassy microdomains of a thermoplastic elastomer, i.e., a poly(styrene-*b*-(ethylene-*alt*-propylene)) (SEP) triblock copolymer. The preferential selectivity of the polystyrene microphase for the oxidant, which does not appear to be achieved in the work by Radhakrishnan and Saini,[9] was accomplished by lightly sulfonating the polystyrene blocks. That sufficiently altered the polarity of the polystyrene, so that aqueous solutions of the

[†] Polymer Science Program.
[‡] Department of Chemical Engineering.

S0024-9297(97)01678-1 CCC: $15.00
Published on Web 03/07/1998

Table 1. Electrical Conductivity of HSEP/PPy Composite Films[a]

sample	wt % PPy	vol % PPy in SPS domains	σ_1 (4-pt probe) (S/cm)	σ_2 (2-pt probe) (S/cm)	σ_1/σ_2
5.6 HSEP35.6	4.8	9.9	7.03×10^{-3} (0.0457)[b]	4.4×10^{-5} (0.6987)[c]	160
7.0 HSEP35.6	6.4	12.8	3.38×10^{-4} (0.0174)	2.9×10^{-5} (0.2828)	12
4.7 HSEP50.4	11.0	15.1	4.42×10^{-2} (0.0006)	4.7×10^{-4} (1.7022)	94
6.0 HSEP50.4	10.0	14.0	1.74×10^{-2} (0.0101)	3.82×10^{-4} (1.8243)	46

[a] Calculated from wt %, assuming all the PPy is in the SPS microphase and $\rho_{SPS} = 1.06$ g/cm^3 and $\rho_{PPy} = 1.35$ g/cm^3. [b] The number in parentheses is the standard deviation of five measurements. [c] The number in parentheses is the standard deviation of three measurements.

oxidant and the pyrrole monomer preferentially partitioned into the sulfonated polystyrene (SPS) microdomains and not into the rubber (EP) microphase. As a result, PPy formation was restricted to the SPS microdomains, which for a lamellar block copolymer texture produced a material in which nanometer-sized lamellae of conductive PPy/SPS were separated by a nanometer-sized EP rubber lamellae.

Experimental Details

The SEP diblock copolymers were synthesized by sequential anionic polymerization of styrene and isoprene, followed by hydrogenation of the polydiene block. Because the polyisoprene microstructure contained essentially 1,4-additions, the resulting rubber block in the hydrogenated SEP was essentially an alternating ethylene−propylene copolymer. The details of the polymerization and hydrogenation reactions, as well as a complete characterization of the block copolymer texture, are given elsewhere.[10] Two different block copolymers were used: one with $M_n = 52$, $M_w/M_n = 1.03$ and containing 35.6 wt % PS and one with $M_n = 52$, $M_w/M_n = 1.04$ and containing 50.4 wt % PS, hereafter referred to as SEP35 and SEP50, respectively. Both exhibited alternating lamellar microstructures in films that were either cast from solution or melt pressed.

The SEP block copolymers were sulfonated using acetyl sulfate following the procedure described by Weiss et al.[11,12] The sulfonation level of the polymer was determined by titration of the sulfonic acid derivatives in a mixed solvent of toluene/methanol (90/10 v/v) to a phenolphthalein end point. Films of sulfonated block copolymers, ca. 200 μm thick, were prepared by slowly evaporating the solvent over a period of 6 days from a partially covered Petri dish containing a 10 wt % solution of the polymer in a toluene/methanol (90/10 v/v) mixed solvent. The cast films were removed from the glass dish and dried at 50 °C under vacuum for at least 48 h and then at 100 °C for 24 h.

The sulfonated diblock copolymers are hereafter denoted as *x.y*HSEP*z*, where *x.y* is the degree of sulfonation of the polystyrene (PS) blocks (mol % styrene sulfonated), H indicates the sulfonic acid derivative, and *z* denotes the nominal wt % styrene, i.e., 35 or 50. For example, 4.7HSEP35 represents the sulfonic acid derivative of a sulfonated diblock copolymer containing 35.6 wt % PS and a degree of sulfonation of 4.7 mol %.

The in situ polymerization of pyrrole in the HSEP films was carried out using the procedure described in ref. 13. The films were first immersed in a 0.5 M aqueous solution of pyrrole for 24 h and then immersed in a 1.0 M aqueous solution of $FeCl_3$ for another 24 h. When the pyrrole polymerization occurred, the films acquired the characteristic black color of PPy. The HSEP/PPy composite film was removed from the $FeCl_3$ solution, washed with distilled water, and dried at 50 °C under vacuum for 48 h. The amount of PPy incorporated in the film was determined gravimetrically.

Dynamic mechanical properties were measured with a Polymer Laboratories MkII dynamic mechanical thermal analyzer (DMTA) using a tensile fixture, a frequency of 1 Hz, a temperature range of −150−200 °C, and a scanning rate of 3 °C/min. Thermal stability of the films was measured with a Perkin-Elmer thermogravimetric analyzer, model TGA-7, using a nitrogen atmosphere and a heating rate of 10 °C/min.

The surface morphology of the films was characterized with an AMR model 1200B scanning electron microscope (SEM) equipped with an EDAX 9100/08 detector and a DX series workstation. EDAX spectra were obtained on samples fractured after immersion in liquid nitrogen. The block copolymer texture was determined with a Philips EM300 transmission electron microscope (TEM) operated at an accelerating voltage of 80 kV. Ultrathin sections were prepared by microtomy using an ultramicrotome LKB Ultratome V equipped with a diamond knife. The sections were collected on Formvar and carbon-coated copper grids and stained at room temperature by exposure to the vapors of a 0.5% aqueous ruthenium tetroxide (RuO_4) solution for 5 min. RuO_4 preferentially stains the polystyrene, thereby enhancing the electron contrast between the two microphases of the block copolymer. Small-angle X-ray scattering (SAXS) measurement experiments were made with a Bonse-Hart camera, equipped with a two-channeled-cut germanium crystal, a scintillation counter and using Cu Kα radiation. All scattering profiles were corrected for sample thickness and absorption.

The dc conductivity of the films (σ_1) was measured by a conventional four-point probe technique in which the electrodes were separated by 0.6 mm; a slight pressure, just enough to ensure a good contact between the film and the four probes, was applied. The bulk conductivity normal to the surface of the film (σ_2) was measured by a two-point probe technique in which the electrodes were firmly pressed against the opposite sides of the film.

Results and Discussion

The HSEP-50 block copolymer ionomer had microstructures consisting of alternating SPS and PEP lamella with a long-spacing determined by SAXS of ∼50 nm.[10] The polymerization of pyrrole occurs only in the presence of oxidant ($FeCl_3$). Because sorption of the aqueous pyrrole and oxidant solutions is much more favorable in the hydrophilic SPS microdomains, as opposed to the hydrophobic rubber microdomains, it was expected that the block copolymer texture would serve as a template for the polymerization and organization of the PPy preferentially within the SPS microdomains.

The HSEP/PPy composites produced are summarized in Table 1. In general, the PPy production increased with increasing polystyrene composition and sulfonation level, which can be attributed to the increased water sorption by the films as the number of sulfonate groups and the volume fraction of the SPS microphase increased. Incorporation of the PPy into the block copolymer had no effect on the thermal stability of the block copolymer. TGA thermographs for the sulfonated diblock copolymers and their composites (not shown) were similar, although the composite exhibited a slower weight loss with increasing temperature that was probably due to the higher viscosity of the composite.

The effect of PPy concentration on the electrical conductivity parallel (σ_1) and perpendicular (σ_2) to the film surface is shown in Figure 1 (note that the lines drawn in Figure 1 serve only to guide the eye and have no real significance). The number of materials studied was not sufficient for determining if there were any intrinsic differences in the conductivities for the com-

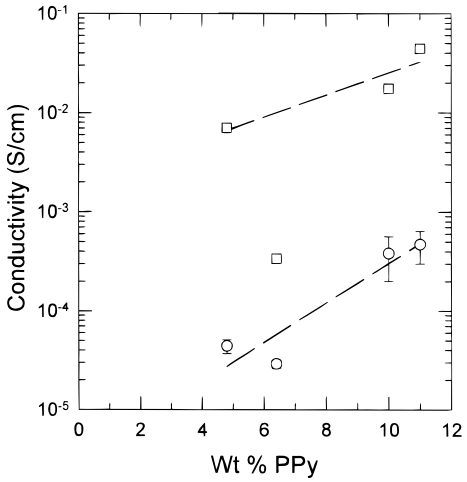

Figure 1. Electrical conductivity of PPy/HSEP nanocomposites: (□) σ_1; (○) σ_2.

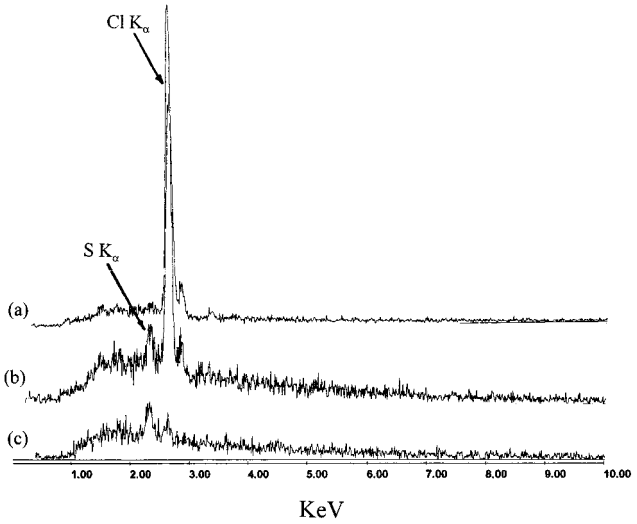

Figure 2. EDAX of the fracture surface of the nanocomposite of 10.0 wt % PPy in 6.0HSEP50: (a) at the surface of the film; (b) at a position intermediate between the surface and center of the film; (c) at the center of the film.

posites prepared from the two different block copolymers. However, because the microstructures of all the materials were similar, i.e., alternating PPy/SPS and EP lamellae, it was assumed that the composition of the block copolymer had a minor effect if any on the electrical properties of the composites.

Both σ_1 and σ_2 increased with increasing PPy concentration, and the conductivity of the composite films was in all cases anisotropic, ranging from 1 to 2 orders of magnitude difference parallel and perpendicular (i.e., σ_1/σ_2) to the film surface. The electrical anisotropy arises from the fact the PPy is preferentially incorporated in the SPS lamella microdomains (the evidence for which will be discussed later in this paper), which for an air-dried film should be preferentially aligned parallel to the film surface. The composite microstructure consisted of conductive SPS/PPy layers separated by nonconducting PEP rubber layers. An ideal microstructure in which the layers are well aligned parallel to the film surface would be expected to have a high conductivity in the plane parallel to the film surface, but little conductivity, i.e., be insulating, perpendicular to the surface. The data in Table 1 and Figure 1, however, show that relatively high conductivity occurred in both planes, which indicates that a conductive PPy pathway was present not only parallel to the film surface but also normal to it. The relatively low electrical anisotropy was due to imperfect alignment of the lamella parallel to the surface of the film. This provided a conductive path both normal to the film surface and in the plane of the film. Still, the higher σ_1 values suggest that there was some preferred orientation of the lamella parallel to the film surface. More details on the microstructure of the nanocomposites are discussed later in this paper.

Conductivity in these composite films occurred at relativity low concentrations of PPy, less than 0.05 mass fraction based on the total mass of the composite (the volume fraction of PPy, though not shown in Table 1, is within 10% of the mass fraction). The percolation threshold concentration for conductivity for a random dispersion of conductive spheres in a polymer is 0.16 volume fraction.[14] For rodlike conductive particles, the threshold concentration is lower,[15,16] though still greater than 0.05 volume fraction. However, nonrandom distributions of a conducting phase in a mixture of conducting and insulating materials can result in conductivity at substantially lower threshold concentrations.[17−19] The unusually high conductivity of the PPy/block copolymer composites at a seemingly low PPy concentration is due to the preferential intercalation of PPy in only the SPS microdomains. As a result, the actual concentration of the conducting polymer within the conducting microphase is much higher, 10−15%, than that based on the total composite mass; see the third column in Table 1.

The conductivity values for the composite film containing 6.4 wt % PPy (see Figure 1) were low compared with the other samples. That was a consequence of the poorer organization of the lamellar microstructure in that sample. Because the PPy is contained only within the SPS domains, the conductivity is sensitive to the texture of the block copolymer microstructure and the long-range order of the microphase-separated domains.

EDAX analyses indicated that Cl^- was the counterion for the protonated PPy and no Fe was detected in the composites, Figure 2. The latter result confirmed that any excess $FeCl_3$ oxidant and the $FeCl_2$ byproduct of the pyrrole polymerization reaction were effectively removed from the composite during the washing process. EDAX measurements of the cross-section of the film near the surface and near the center indicated, however, that the Cl^- concentration (see the Cl K_α peak in Figure 2), and presumably the PPy concentration as well, was higher near the surface.

The inhomogeneous distribution of PPy through the film thickness is not surprising in that the pyrrole polymerization reaction was accomplished by diffusing the oxidant into a pyrrole-swollen film. Because the oxidant diffuses from the surface into the film and the polymerization reaction occurred where both oxidant and pyrrole were present, the polymerization actually occurs from the surface of the film inward. The S K_α, which is due to the sulfonate groups of the ionomer microphase, is suppressed in the EDAX of the surface region, which indicates a relatively high concentration of PPy at the surface—that is, a low concentration of the block copolymer. One explanation for the PPy gradient in the film is that polymerization of pyrrole retarded or inhibited the diffusion of the oxidant solution into the film, so that the reaction did not occur

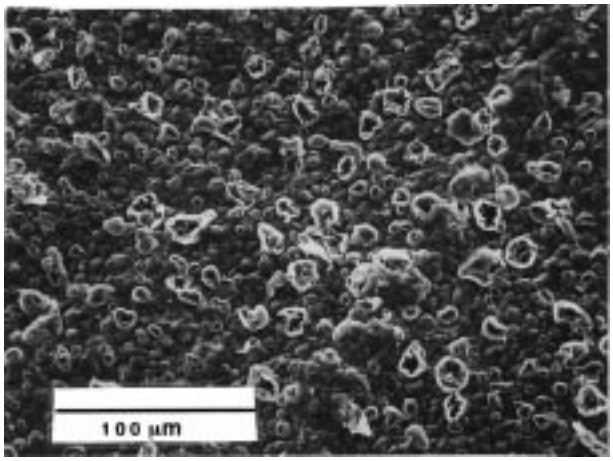

Figure 3. SEM micrograph of the surface of a nanocomposite film of 4.8 wt % PPy in 5.6HSEP35.

uniformly throughout the film. This is manifest by a depletion of PPy at the center of the film. The PPy concentration in the film generally increased with increasing sulfonation level and volume of the sulfonated microphase, and EDAX indicated that more PPy penetrated into the core of the film as the total PPy concentration increased.

Figure 3 is an SEM micrograph of the surface of the 5.6HSEP35.6 composite (4.8% PPy). The micrograph clearly shows 5−20 μm PPy particles on the surface, though they appear to be embedded in the film rather than simply deposited on the surface. There was no noticeable debris on the surface by visual observation of the films, and the films were not freely marking. Those observations are consistent with PPy particles being embedded in the polymer. No PPy phase was observed by SEM in fracture surfaces of the film, other than at the film surface. Because the EDAX analyses indicated that the PPy was present in the core, as well as on the surface, it would appear that PPy was incorporated in the core on a size scale smaller than the resolution of the SEM (<0.1 μm). The PPy particles observed on the surface of the composite films may contribute in part to the electrical anisotropy. However, the PPy surface layer cannot explain the relatively high conductivity (10^{-5}−10^{-3} S/cm) normal to the film surface. If the PPy were homogeneously dispersed within the bulk of the film, the concentration of PPy in the bulk phase would be too low to provide a percolation pathway for conductivity, and the conductivity should be $<10^{-8}$ S/cm. The only way that conductivity could occur normal to the film surface in these samples is if the PPy were concentrated within one of the microphases.

A comparison of TEM micrographs before and after the in situ polymerization of pyrrole in the 5.6HSEP35.6 block copolymer indicated that PPy was intercalated within the 10−20 nm thick SPS lamellae of the block copolymer, Figure 4. The PPy/5.6HSEP35.6 sample contained 4.8% (wt) PPy. The dark microphase in Figure 4 corresponds to the RuO_4-stained SPS lamellae and the lighter domains are the EP rubber lamellae. It is clear that the in situ polymerization of pyrrole did not perturb the general block copolymer texture, though the interface between the lamellae is not as sharp in the composite as in the neat block copolymer. Evidence for the preferential segregation of the PPy into the SPS domains can be inferred from the preservation of the contrast between the microphases in the TEM micrographs in Figure 4. Since RuO_4 is expected to react with the double bonds of the PPy, as well as with the styrene, the EP microphase should also be stained if it contained appreciable PPy. The swelling of the SPS lamellae also indicated that the PPy was in those microdomains.

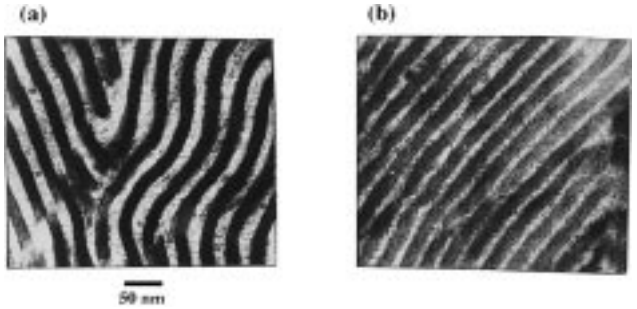

Figure 4. TEM micrograph of cross-section of films of (a) 5.6HSEP35.6 and (b) nanocomposite of 4.8 wt % PPy in 5.6HSEP35. The dark regions are the SPS microphase.

Table 2. Microstructure Period for the Block Copolymer and Thickness of the SPS Lamellae Measured by SAXS and TEM

				SAXS		TEM	
sample	PPy wt %	ϕ_2	q (nm^{-1})	D (nm)	L (nm)	D (nm)	L (nm)
5.6HSEP35.6	0	0.334	0.111	56.7	18.94	32.6	10.9
5.6HSEP 35.6	4.8	0.355	0.114	55.1	19.56	33.7	12
7.0HSEP35.6	0	0.334	0.141	44.6	14.9	28.1	9.4
7.0HSEP35.6	6.4	0.367	0.142	44.1	16.18	26.4	9.7
4.7HSEP50.4	0	0.480	0.145	43.2	20.74	24.7	11.9
4.7HSEP50.4	11	0.519	0.144	43.7	22.68	28.1	14.6
6.0HSEP50.4	0	0.480				24.7	11.9
6.0HSEP50.4	10	0.520				28.1	14.6

The characteristic distance of the lamellar texture, measured from the center-to-center spacing of two consecutive SPS lamellae, increased upon incorporation of PPy into the block copolymer; see Table 2. Within the experimental error associated with measuring lamellae thickness from the micrographs, an increase in the thickness of the SPS lamellae accounted for the increased domain spacing; see Table 2. Similar results were obtained from TEM analysis of the other composites, though in some cases, the long-range order of the lamellae was not as pronounced as for the sample in Figure 4. However, in each case, except for the swelling of the SPS domain thickness and the development of a more diffuse interface between lamellae, the block copolymer textures of the composites were comparable to those of the original block copolymer film.

Figure 5 is a TEM micrograph of a cross-section of a nanocomposite of 6.4 wt % PPy in 7.0HSEP35.6. This was the sample that had the lowest anisotropy of the conductivity; see Figure 1. The reason for the high σ_2 is evident from the poor alignment of the lamellae microphases in this sample (cf. Figures 4 and 5), which provide a conductive PPy/SPS pathway normal, as well as parallel, to the surface of the film.

A SAXS profile for the nanocomposite of 5.6HSEP35.6 containing 4.2 wt % PPy is shown in Figure 6. Six scattering peaks are visible (see arrows), and the ratio of the scattering vectors, q, of the maxima ($q = 4\pi(\sin\theta)/\lambda$, where θ is half the scattering angle and λ is the X-ray wavelength) correspond approximately to 1:2:3:4:5:6, which is characteristic of a lamellar structure. Some uncertainty in the position of the scattering maxima with respect to the first maximum arises from the desmearing procedure, which probably explains the

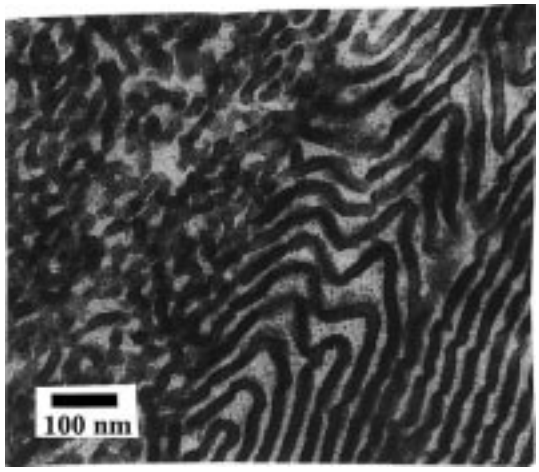

Figure 5. TEM micrograph of cross-section of a nanocomposite film of 6.4 wt % PPy in 7.0HSEP35.6.

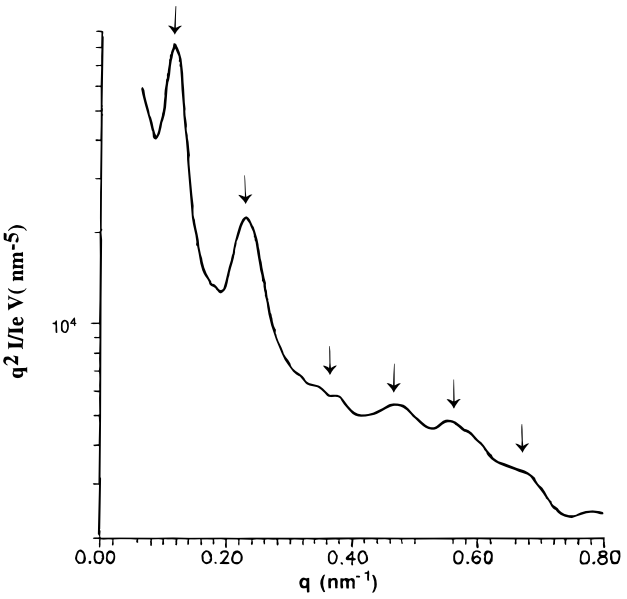

Figure 6. SAXS profile a nanocomposite film of 4.2 wt % PPy in 5.6HSEP35.6. The incident beam was normal to the surface of the film.

deviation of the peak positions from integer multiples of q from the first maximum. The third- and sixth-order maxima in Figure 6 are suppressed as a consequence of selective interference with the particle shape factor of the lamellar stacks, which suppresses the SAXS maxima of $\sim 1/w_{SPS}$, where w_{SPS} is the mass fraction of the ionomeric block.[20] SAXS profiles corresponding to lamellar microstructures were also obtained for the other block copolymer and nanocomposite films used in this study, except in some cases only the first and second maxima were observed due to poorer development of the texture and less long-range order in those films.

The position of the first-order maximum in the SAXS curve, q^*, provides an estimate of the period of the lamellar structure, D, by applying Bragg's law:

$$D = 2\pi/q^* \quad (1)$$

The thickness of the ionomer lamellae, L, was calculated from

$$L = D\phi_2 \quad (2)$$

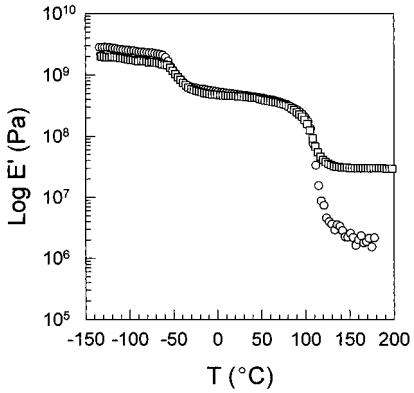

Figure 7. Dynamic modulus vs temperature for films of (○) 4.7HSEP50 and (□) nanocomposite of 11 wt % PPy in 4.7HSEP50.

where ϕ_2 is the volume fraction of the sulfonated block. The results for these two calculations are given in Table 2 for the neat block copolymers and the composites. ϕ_2 for the composite films was calculated by assuming that all the PPy was in the SPS microdomains and that the density of the PPy-containing ionomer phase was a weighted average of the densities of the two polymers. Although the absolute value of D and L calculated from the SAXS and TEM data differed, in both cases the lamellae thickness of the SPS lamellae increased with incorporation of PPy. The discrepancy of the lengths measured by the two techniques may be partially due to some of the assumptions inherent in the sizes calculated from the SAXS data and to the errors in measuring the lamellae thickness off the micrograph.

The dynamic storage modulus, E', is plotted against temperature in Figure 7 for 4.7HSEP50 and a composite containing 11 wt % PPy. The two transitions, at ca. −50 °C and ca. 110 °C, are the glass transition temperatures of the PEP and SPS microphases, respectively. The T_g of the SPS phase in the nanocomposite was slightly lower than that for the neat block copolymer, which may be due to either plasticization by residual water or disruption of the hydrogen-bonded network of sulfonic acid groups by intermolecular hydrogen bonding of the PPy and the ionomer.

The major influence of the incorporation of PPy on the viscoelastic behavior of the block copolymer ionomer was to increase E' above the T_g of the SPS microphase. That was a result of the rigid PPy serving as a reinforcement for the block copolymer melt. The modulus enhancement at elevated temperature was more than 1 order of magnitude, and no viscous flow of the block copolymer composite was observed up to 200 °C. A similar enhancement of E' above T_g by the incorporation of PPy by an in situ polymerization of pyrrole was previously reported for an SPS ionomer.[13] The other PPy-containing block copolymers exhibited similar behavior, though the magnitude of the reinforcement above T_g of the SPS microphase depended upon the PPy concentration. The differences in the modulus of the two materials below T_g of the PEP microphase, i.e., $T < -50$ °C, are probably due to slippage of the glassy film in the test fixture and are not considered significant.

Conclusions

Ionomeric block copolymers, sulfonated poly(styrene-*b*-(ethylene-*co*-propylene), with alternating lamella mi-

crodomains were used as templates for the in situ polymerization of pyrrole. The reaction locus for the polymerization was the hydrophilic sulfonated polystyrene microdomains, which were preferentially swollen by aqueous solutions of the pyrrole monomer and the $FeCl_3$ oxidant.

Incorporation of PPy did not affect the alternating lamellae microstructure of the block copolymer, though the boundaries between the polystyrene and rubber microphase became more diffuse. Both the surface and bulk conductivity were dependent upon the amount of PPy incorporated into the system; conductivity parallel to the film surface varied from 10^{-3} to 10^{-1} S/cm as the PPy concentration varied from 5 to 11 wt %. The conductivity normal to the surface was generally 1−2 orders of magnitude lower. Presumably, samples with higher anisotropy of the conductivity could be prepared if the alignment of the microstructure were improved. Incorporation of PPy into the block copolymer also improved the modulus of the melt above the T_g of the SPS microdomains and suppressed viscous flow of the composite.

Acknowledgment. This work was partially funded by grants from the Army Research Office (Grant DAAH 04-94-G-0082) and by Connecticut Innovations Inc. (Grant 95G022). We are grateful to Dr. Benjamin Hsiao at the DuPont Central Research and Development Laboratory for the SAXS results and Prof. Marie Cantino and Dr. Lamia Khairallah of the Electron Microscopy Laboratory in the Department of Physiology and Neurobiology at the University of Connecticut for the TEM micrographs.

References and Notes

(1) De Jesus, M. C.; Fu, Y.; Weiss, R. A. *Polym. Eng. Sci.* **1997**, *37*, 1936.
(2) Bates, F. S.; Fredrickson, G. H. *Annu. Rev. Phys. Chem.* **1990**, *41*, 525.
(3) Ishizu, K.; Yamada, Y.; Fukutomi, T. *Polymer* **1990**, *31*, 2047.
(4) Ishizu, K.; Yamada, Y.; Saito, R. ; Kanbara, T.; Yamamoto, T. *Polymer* **1992**, *33*, 1816.
(5) Ishizu, K.; Yamada, Y.; Saito, R. ; Kanbara, T.; Yamamoto, T. *Polymer* **1992**, *34*, 2256.
(6) Stankovic, R. I.; Lenz, R. W.; Karasz, F. *Eur. Polym. J.* **1990**, *26*, 3.
(7) Ishizu, K.; Honda, K.; Kanbara, T.; Yamamoto, T. *Polymer* **1994**, *35*, 22.
(8) Smith, R. C.; Fischer, W. M.; Gin, D. I. J. *Am. Chem. Soc.* **1997**, *119*, 4092.
(9) Radhakrishnan, S.; Saini, D. R. *Polym. Int.* **1994**, *34*, 1.
(10) Mani, S.; Weiss, R. A.; Hahn, S. F.; Williams, C. E.; Cantino, M. E.; Khairallah, L. H. *Polymer*, in press.
(11) Weiss, R. A.;. Sen, A.; Pottick, L. A.; Willis, C. L. *Polymer Commun.* **1990**, *31*, 220.
(12) Weiss, R. A.;. Sen, A.; Pottick, L. A.; Willis, C. L. *Polym.* **1991**, *32*, 1867.
(13) De Jesus, M. C.; Weiss, R. A.; Chen, Y. *J. Polym. Sci. Part B: Polym. Phys.* **1997**, *35*, 347.
(14) Zallen, R. *The Physics of Amorphous Solids*; John Wiley: New York, 1983; Chapter 4.
(15) Andreatta, A.; Heeger, A. J.; Smith, P. *Polym. Commun.* **1990**, *31*, 275.
(16) Balberg, I.; Anderson, C. H.; Alexander, S.; Wagner, N. *Phys. Rev. B* **1984**, *30*, 3933.
(17) Levon, K.; Margolina, A.; Patashinsky, A. *Macromolecules* **1993**, *26*, 4061.
(18) Wang, Y.; Rubner, M. F. *Macromolecules* **1992**, *25*, 3284.
(19) Yang, C. Y.; Cao, Y.; Smith, P.; Heeger, A. J. *Synth. Met.* **1993**, *53*, 293.
(20) *Small Angle X-ray Scattering*; Glatter, O., Kratky, O., Eds.; Academic Press: New York, 1982.

MA971678A